ISSN:2523 - 0522
Volume 8, Issue 2, October 2025
ISRAA UNIVERSITY JOURNAL OF APPLIED SCIENCE (IUJAS)

ORIGINAL ARTICLE

Structural Assessment of Basketball Court Concrete Using Impact-Echo and Phase Angle Analysis

Sameh Fuqaha[1], Muhamad Umam[1] , Septya Salsalbilla[1] , Ahmad Zaki*[2] , Sri Atmaja[2], Guntur Nugroho[2]

Received:13/07/2025 ***Accepted:08/09/2025*** ***Published: 01/10/2025***

OPEN ACCESS

Doi: https://doi.org/10.52865/IUYZ8061

Competing Interests:
The authors declare that this manuscript was approved by all authors in its form and that no competing interest exists.

Affiliation and Correspondence:

1. Postgraduate Studies, Department of Civil Engineering, Universitas Muhammadiyah Yogyakarta, Yogyakarta, Indonesia.
2. Department of Civil Engineering, Faculty of Engineering, Universitas Muhammadiyah Yogyakarta, 55183, Yogyakarta, Indonesia.

***Corresponding Author Email:**

ahmad.zaki@umy.ac.id

ABSTRACT:

Background*: The structural integrity of basketball court concrete is critical for both safety and performance, yet systematic nondestructive evaluation (NDE) studies on thin-slab sports flooring remain limited. This research addresses that gap by applying the Impact-Echo (IE) method to assess material uniformity and detect potential flaws in basketball court concrete. Unlike most prior studies that emphasize frequency-domain analysis, this study integrates both Fourier Transform and Phase Angle behavior to enhance diagnostic reliability.*

Methods: *Experimental testing was conducted with small and large hammers at sensor spacings of 10, 20, and 30 cm along three parallel lines of a full-scale court. Signals were processed using Fast Fourier Transform (FFT) and Phase Angle analysis to identify dominant frequency peaks, calculate thickness, and evaluate wave coherence.*

Results: *Results show a clear inverse correlation between frequency and slab thickness, with Line 3 exhibiting the highest uniformity and Line 1 indicating localized variability. Phase Angle analysis revealed strong sensitivity to sensor distance and hammer size: small hammers with short spacing captured fine-scale anomalies, while large hammers and wider spacing yielded smoother generalized responses. To our knowledge, this is among the first studies to systematically evaluate basketball court concrete using both Fourier and Phase Angle analysis across varied sensor and hammer configurations.*

Conclusion: *The findings refine understanding of how test parameters influence IE outcomes in thin concrete layers and provide a foundation for standardized, reliable NDE protocols that support quality control, safety assurance, and long-term monitoring of sports infrastructure.*

KEYWORDS: Impact-Echo (IE), basketball court concrete, nondestructive evaluation, phase angle analysis, structural integrity.

INTRODUCTION:

The Impact-Echo (IE) method has emerged as a cornerstone in the field of nondestructive evaluation (NDE), particularly for assessing the internal condition and structural integrity of concrete systems. By analyzing transient stress waves generated through mechanical impacts, IE testing allows for the identification of subsurface anomalies such as voids, cracks, and delaminations without inflicting any damage on the tested material. These resonance-based analyses have demonstrated high effectiveness in estimating both the presence and depth of internal flaws (Sengupta et al., 2024). Furthermore, the method has proven capable of characterizing critical material properties such as stiffness and density, making it a reliable and cost-efficient alternative to destructive techniques like core sampling and drilling (Kim et al., 2022).

Advancements in signal processing and instrumentation have significantly enhanced the diagnostic capabilities of the IE method. Techniques such as Short-Time Fourier Transform (STFT) and wave-equation-based modeling have improved time-frequency resolution, effectively reduced noise interference and facilitating the accurate detection of subtle structural anomalies . Additionally, the integration of multi-transducer arrays and non-contact impact sources has extended the method's applicability to a wide range of structural settings, including pavements, bridge decks, and foundation systems (Sawicki et al., 2021; Yu et al., 2022).

IE testing has also been employed in complex; multilayered systems where heterogeneous materials and boundary conditions pose challenges to traditional methods. In such contexts, the technique has shown promise when combined with other NDE approaches, such as Ultrasonic Pulse Velocity (UPV) and Ground-Penetrating Radar (GPR) (Dethof et al., 2024). These hybrid applications have facilitated more holistic evaluations, especially in infrastructure types like railway slabs and tunnel linings (Dvořák & Topolář, 2021; Ge et al., 2022; Scherr & Grosse, 2021). Notably, the reliability of the IE method has also been validated under extreme environmental conditions, including freeze-thaw cycles and elevated moisture levels, reinforcing its robustness in diverse operational environments (Wang & Gupta, 2021).

The integration of machine learning into IE data interpretation has further enhanced the technique's utility, enabling automated flaw detection with improved accuracy and scalability for large-area assessments (Apostolopoulos, 2010; Lu et al., 2021). However, despite these technological advancements, the application of IE testing to sports infrastructure such as basketball courts has

received comparatively limited research attention.

In the context of sports flooring, structural integrity and material uniformity are essential for both athlete safety and surface performance (Afanda & Zaki, 2025). Thin concrete slabs, often used in sports courts, require fine-tuned testing methodologies to ensure effective flaw detection. Recent studies have begun to address these challenges by refining IE testing parameters such as hammer type, sensor spacing, and line alignment (Kouddane et al., 2022). For instance, blunt-tipped hammers have been shown to generate more consistent impact signals, making them more suitable for evaluating thin concrete layers (Dvořák & Topolář, 2021). Furthermore, the application of Phase Angle Analysis and advanced tools like the Fast Fourier Transform (FFT) has improved the clarity and interpretability of frequency-time data, enabling more accurate identification of subsurface defects (Kee et al., 2020; Lin & Ye, 2019).

Nevertheless, there remains a significant research gap regarding the detailed assessment of basketball court concrete, particularly with respect to the combined effects of testing parameters on anomaly detection. Most prior investigations have emphasized frequency-domain analysis, while the role of Phase Angle behavior in material consistency evaluation has been underexplored. Moreover, comprehensive studies addressing how sensor distance, hammer size, and line orientation jointly influence IE results in thin-slab sports surfaces are lacking. This study seeks to fill these knowledge gaps by applying the Impact-Echo method to systematically evaluate the structural and material properties of basketball court flooring.

The research focuses on the influence of sensor configuration, hammer characteristics, and test alignment on the resulting frequency and phase behavior. By correlating dominant frequency peaks with concrete thickness and analyzing Phase Angle variations, this study aims to uncover subtle indicators of material heterogeneity and potential flaws. To our knowledge, this is among the first studies to systematically evaluate basketball court concrete using both Fourier and Phase Angle analysis across varied sensor and hammer configurations. Ultimately, the research strives to refine and optimize IE testing protocols for more precise and reliable assessments of sports infrastructure, with the final objective of establishing practical guidelines for nondestructive evaluation and long-term monitoring of sports flooring systems.

METHODS and MATRRIALS

This study employed a comprehensive nondestructive testing (NDT) approach to evaluate the material properties and structural integrity of a basketball court using the Impact-Echo (IE) method. Both small and big hammers were utilized to generate mechanical impulses, allowing the characterization of different wave behaviors. Table 1 summarizes the Impact-Echo test configurations, combining hammer type, sensor distance, and applied lines. The integration of Fast Fourier Transform (FFT) and Phase Angle analyses facilitated a detailed interpretation of the acquired data. This enabled the identification of dominant frequency peaks and structural inconsistencies, contributing to a deeper understanding of material uniformity across the court surface. By systematically varying hammer size and sensor distance, the study explored their influence on signal sensitivity and defect detection accuracy.

Table 1. Summary of Test Configurations for Impact-Echo Measurements

Hammer Type	**Sensor Distances (cm)**	**Applied Test Lines**	**Purpose / Expected Response**
Small Hammer	10, 20, 30	Lines 1, 2, 3	High-frequency, localized responses; sensitive to surface variations and fine-scale anomalies
Big Hammer	20, 30	Lines 1, 2, 3	Low-frequency, broader responses; deeper penetration and generalized structural assessment

Study Site

The experimental investigation was carried out on a basketball court located within the campus of Universitas Muhammadiyah Yogyakarta (UMY), Indonesia. This site was selected for its accessibility, controlled testing environment, and typical representation of concrete flooring used in sports infrastructure (Figure 1). The open layout of the court, surrounded by campus streets and laboratories, introduced occasional environmental noise, which was carefully considered during data analysis to ensure signal clarity and reliability.

Experimental Setup

The experimental configuration (Figure 3) consisted of a manually operated impact hammer and two piezoelectric sensors positioned on the concrete surface to record wave responses. The sensors were connected to a NI-USB-4432 data acquisition system (DAQ), ensuring high-fidelity signal capture and accurate temporal resolution (Figures 4 and 5).

ISSN:2523 - 0522
Volume 8, Issue 2, October 2025
ISRAA UNIVERSITY JOURNAL OF APPLIED SCIENCE (IUJAS)

Two types of impact hammers were employed during testing (Figure 6). The small hammer, designed to produce short-duration, high-frequency signals, was optimal for detecting fine structural variations. The big hammer, producing lower-frequency, longer-duration impulses, was suited for assessing broader material behavior and deeper flaw penetration.

Testing Lines and Configurations

The testing was conducted along three distinct lines on the basketball court to ensure a comprehensive evaluation of the surface as shown in Figure 7. The central line was positioned at the center of the court, serving as the primary reference line. The line above was located 15 cm above the central line, while the line below was positioned 15 cm below the central line. This arrangement enabled the assessment of material properties and wave propagation behavior across different areas of the court.

Figure 1. Study site: Basketball court location used for Impact-Echo testing

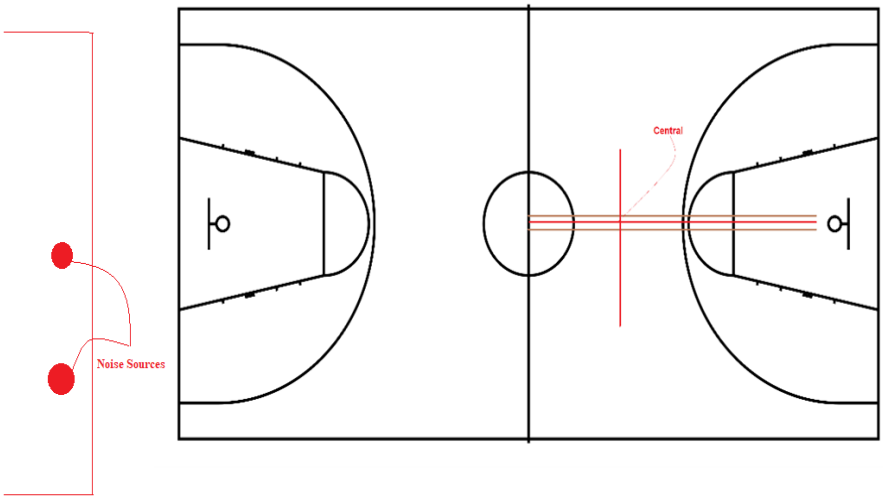

ISSN:2523 - 0522
Volume 8, Issue 2, October 2025
ISRAA UNIVERSITY JOURNAL OF APPLIED SCIENCE (IUJAS)

Figure 2. Noise sources affecting Impact-Echo testing in outdoor basketball courts

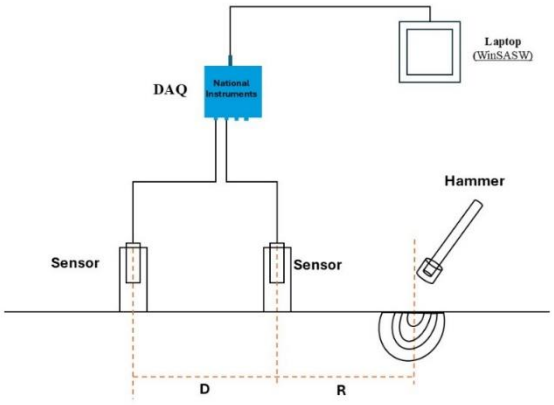

Figure 3. Schematic of the Impact-Echo test setup

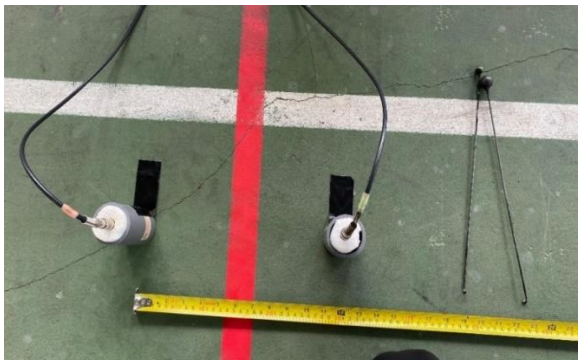

Figure 4. Close-up view of the piezoelectric sensors used for data collection.

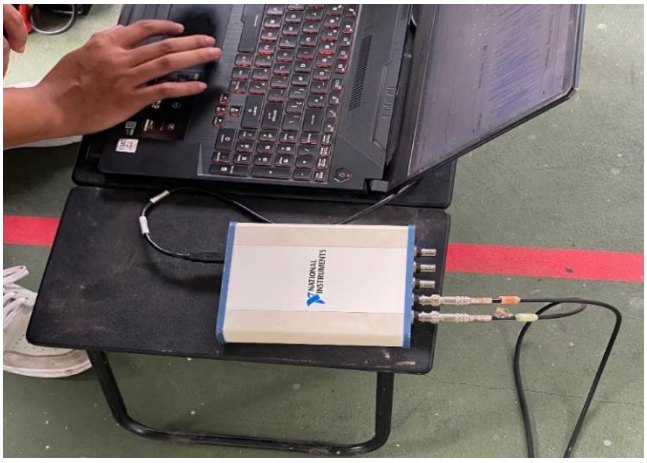

Figure 5. Impact-Echo signal acquisition system (NI-USB-4432 model)

ISSN:2523 - 0522
Volume 8, Issue 2, October 2025
ISRAA UNIVERSITY JOURNAL OF APPLIED SCIENCE (IUJAS)

Figure 6. Impact hammers used in the experiment (small and big).

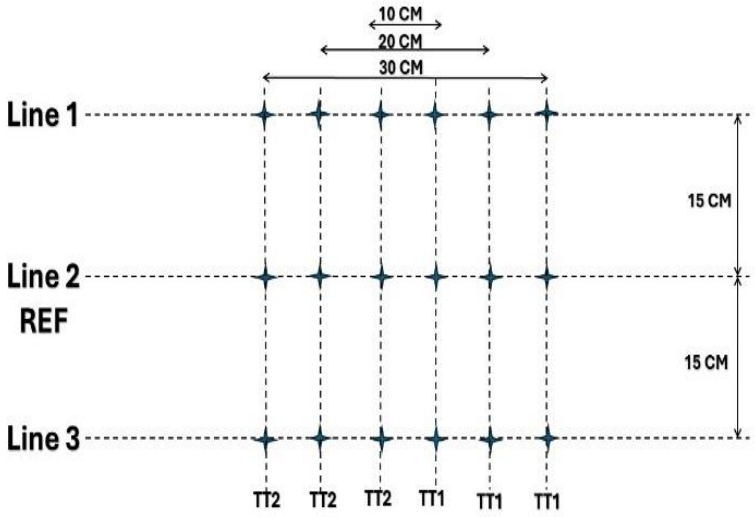

Figure 7. Testing configuration showing three parallel lines (Central, Above, and Below).

To evaluate wave propagation over varying distances, specific sensor spacings were utilized for each hammer type. For the small hammer, sensor spacings of 10 cm, 20 cm, and 30 cm were used to capture high-frequency, localized responses, while for the big hammer, spacings of 20 cm and 30 cm were selected to focus on broader, low-frequency wave behavior. This systematic approach ensured that the analysis accounted for the effects of both hammer type and sensor distance on the structural response, as summarized in Table 1.

Data Analysis

The collected vibrational data were systematically analyzed in both the time and frequency domains to evaluate the structural characteristics and uniformity of the basketball court surface (Figure 8). Initial data processing was performed using WinSASW software, a specialized tool for surface wave analysis. WinSASW employs an algorithm based on the stiffness matrix approach (Joh, 1996), enabling

the generation of theoretical dispersion curves from input shear wave velocity profiles.

This software facilitated the transformation of raw time-domain signals into the frequency domain and supported the construction of dispersion curves across different sensor spacings. A key component of this process involved inversion analysis, whereby theoretical curves were iteratively adjusted to match the experimental data. This procedure yielded an accurate estimation of shear wave velocity profiles, providing valuable insights into the mechanical behavior of subsurface concrete layers. After processing in WinSASW, the data were exported into Microsoft Excel, where amplitude versus time values were extracted and organized for further analysis. This allowed for detailed comparison across configurations involving different hammer sizes and sensor spacings (Bogolyubsky et al., 2021).

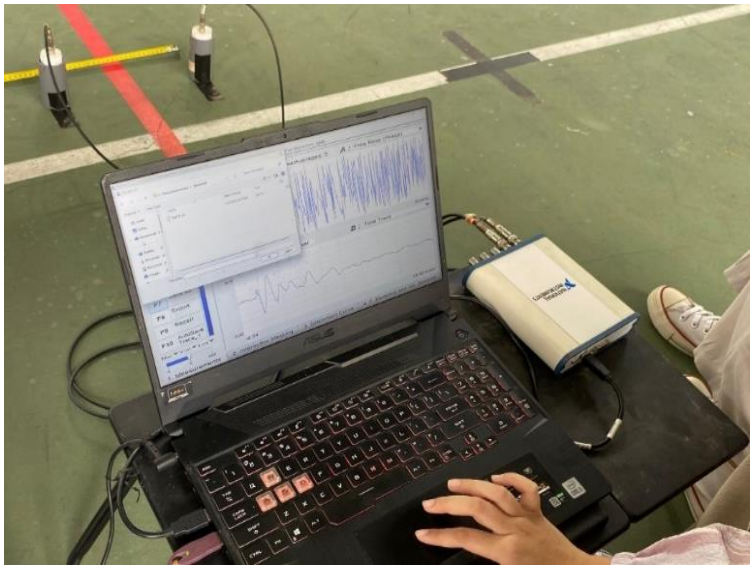

Figure 8. Workflow for Impact-Echo data processing, including Fourier Transform and Phase Angle analysis

Fourier Transform (FT) analysis was employed to explore the frequency spectra of the recorded signals, with particular emphasis on identifying dominant frequency peaks that characterize the structural response of the concrete. These peaks correspond to specific resonant modes and reveal key features of the material, including layer thickness, stiffness variations, and the presence of subsurface anomalies.

To complement the spectral analysis, Phase Angle Analysis was conducted to assess wave coherence and propagation behavior under varying test conditions. By examining the phase relationships

between sensor recordings, this analysis provided deeper insight into material dispersion, revealing potential irregularities arising from heterogeneous concrete composition, delaminations, or voids. All frequency and phase data were visualized using Python-based graphical plots to enhance the clarity and interpretation of structural behavior across configurations.

The Fourier Transform and Phase Angle analyses were initially processed using Microsoft Excel, while advanced visualizations were generated using Python. Python's computational tools enabled the creation of clear and precise graphical representations of both frequency spectra and phase angle behavior, enhancing the accuracy and interpretability of the results. To further evaluate the structural characteristics of the basketball court, the thickness of the concrete layer was calculated using Equation (1) (Sansalone & Streett, 1997).

$$T = \frac{V}{2f} \quad (1)$$

Where T is the material thickness (m), V is the wave velocity (m/s), f is the dominant frequency (Hz). This formula was applied to the frequency-domain data obtained through WinSASW software, enabling the accurate estimation of concrete thickness across different test points. The correlation between dominant frequency and material thickness provided meaningful insight into the uniformity and potential variability of subsurface conditions across the tested configurations.

This methodology ensured a detailed evaluation of the basketball court's material properties by utilizing both small and big hammers to capture a wide range of wave characteristics. Sensor distances of 10 cm, 20 cm, and 30 cm were employed to assess both high-frequency localized responses and low-frequency broad-spectrum behavior. The combined use of Fourier Transform and Phase Angle analyses offered a comprehensive view of material uniformity, allowing for the identification of dominant frequencies and assessment of structural consistency. These analytical techniques highlighted the influence of sensor spacing and hammer size on the accuracy and sensitivity of defect detection, offering valuable insights into the court's material variability.

RESULTS and DISCUSSION

The Analysis and Findings section presents the outcomes of the Impact-Echo (IE) testing conducted on a basketball court surface, aimed at evaluating its structural integrity and material uniformity. Data were collected using both small and big hammers across sensor distances of 10 cm, 20 cm, and 30 cm,

ISSN:2523 - 0522
Volume 8, Issue 2, October 2025
ISRAA UNIVERSITY JOURNAL OF APPLIED SCIENCE (IUJAS)

and subsequently analyzed using Fourier Transform and Phase Angle techniques.

By examining the vibrational responses obtained along three distinct test lines Central Line, Line Above, and Line Below the analysis identifies key trends in frequency distribution, investigates material homogeneity, and evaluates the influence of testing configurations on the reliability of subsurface assessments. The findings contribute to a deeper understanding of the structural health of the concrete surface and help to pinpoint areas of inconsistency or potential deterioration.

Fourier Transform analysis

The Fourier Transform analysis of the vibrational data from the three testing lines provided detailed insights into the frequency characteristics, material properties, and wave propagation behavior of the basketball court surface. Using both small and big hammers, and varying the sensor spacing (10 cm, 20 cm, and 30 cm), frequency spectra were generated for each configuration. Figures 9, 10, and 11 illustrate the frequency distribution spectra corresponding to different test conditions. Each spectrum displays clear dominant frequency peaks, which are essential in evaluating the thickness and stiffness of the concrete layer. Higher dominant frequencies were generally associated with thinner or stiffer surface regions, while lower frequencies indicated potential variability or reduced stiffness.

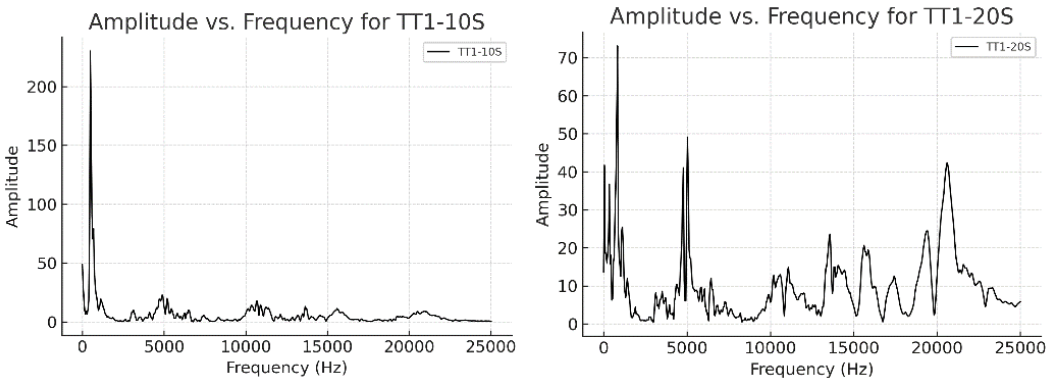

ISSN:2523 - 0522
Volume 8, Issue 2, October 2025
ISRAA UNIVERSITY JOURNAL OF APPLIED SCIENCE (IUJAS)

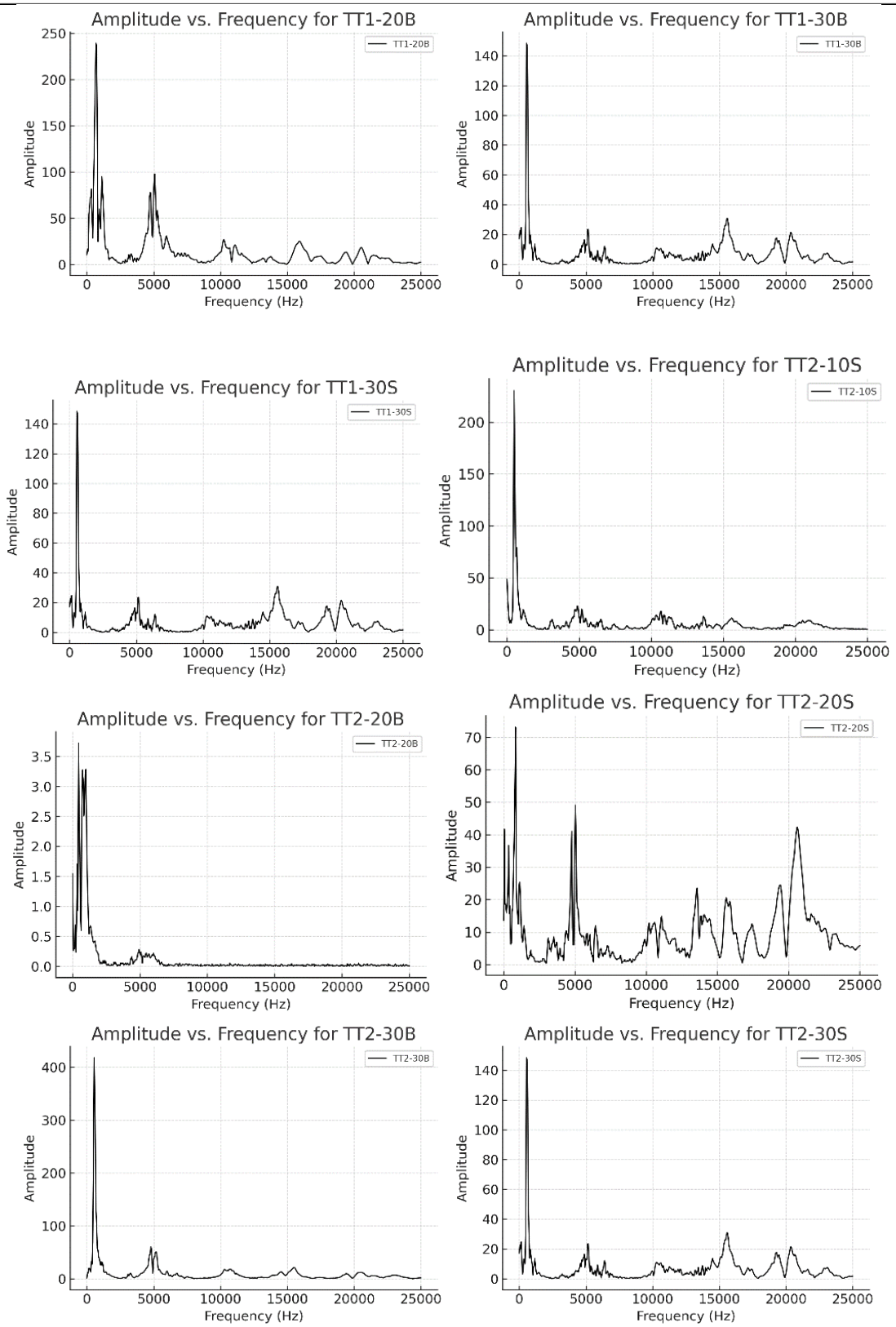

Figure 9. Amplitude vs. frequency spectrum for Line 1

ISSN:2523 - 0522
Volume 8, Issue 2, October 2025
ISRAA UNIVERSITY JOURNAL OF APPLIED SCIENCE (IUJAS)

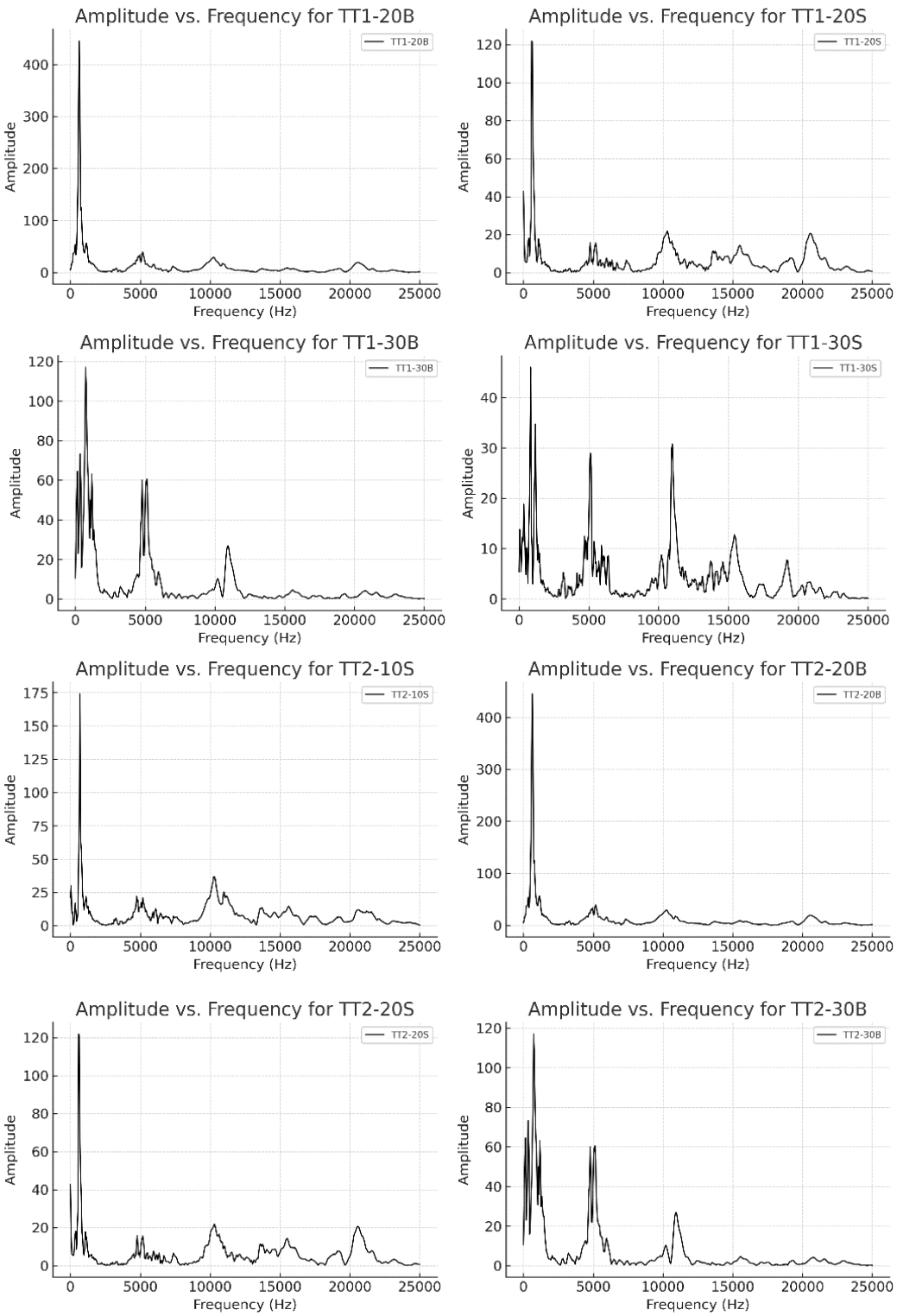

ISSN:2523 - 0522
Volume 8, Issue 2, October 2025
ISRAA UNIVERSITY JOURNAL OF APPLIED SCIENCE (IUJAS)

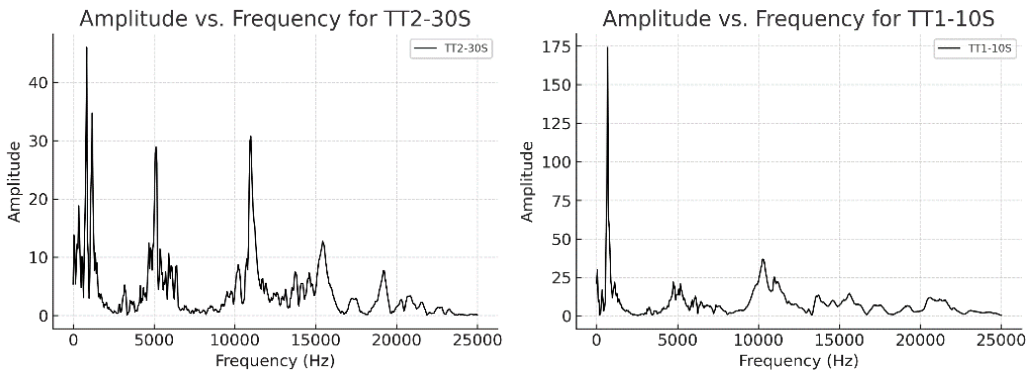

Figure 10. Amplitude vs. frequency spectrum for Line 2.

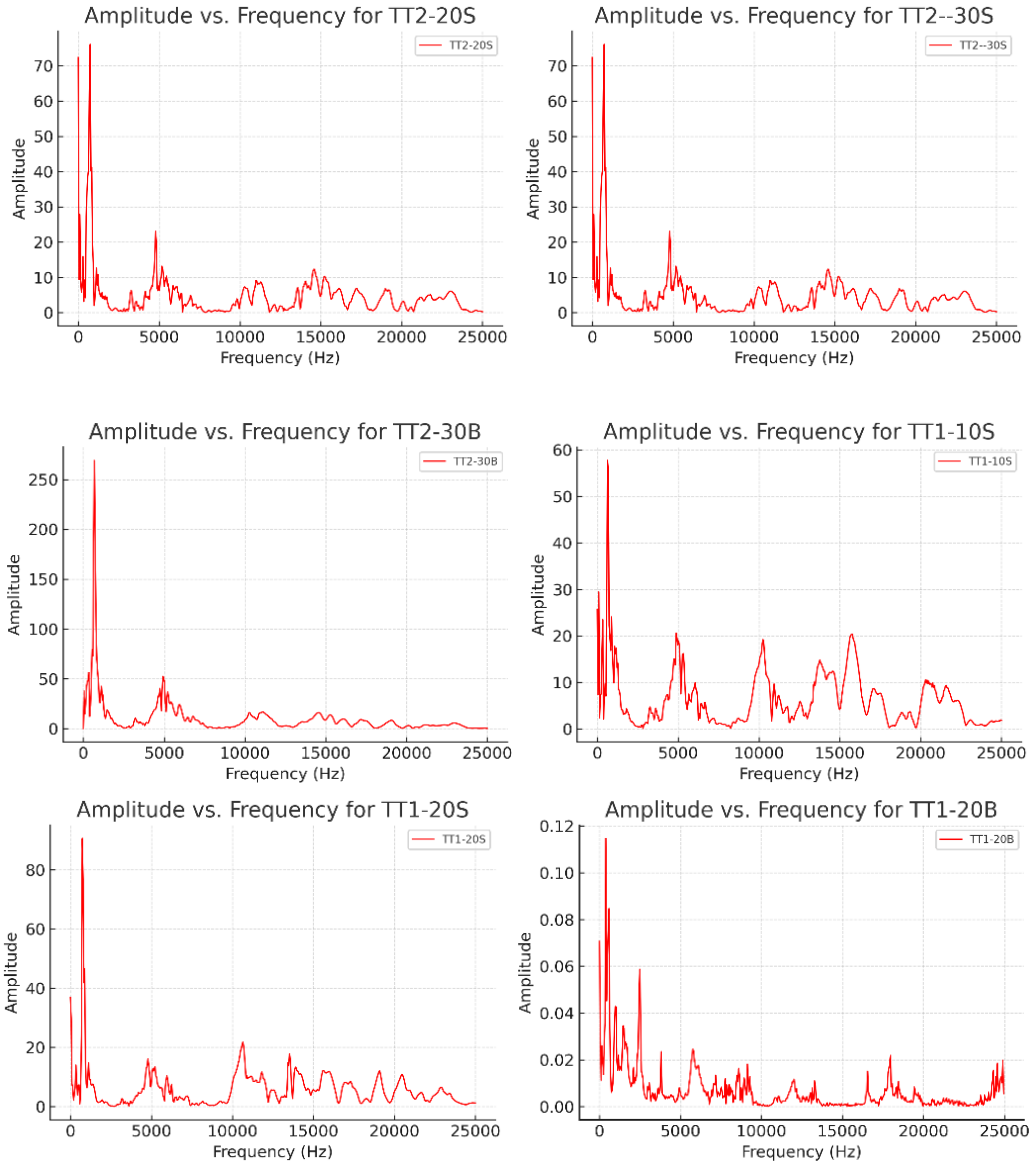

ISSN:2523 - 0522
Volume 8, Issue 2, October 2025
ISRAA UNIVERSITY JOURNAL OF APPLIED SCIENCE (IUJAS)

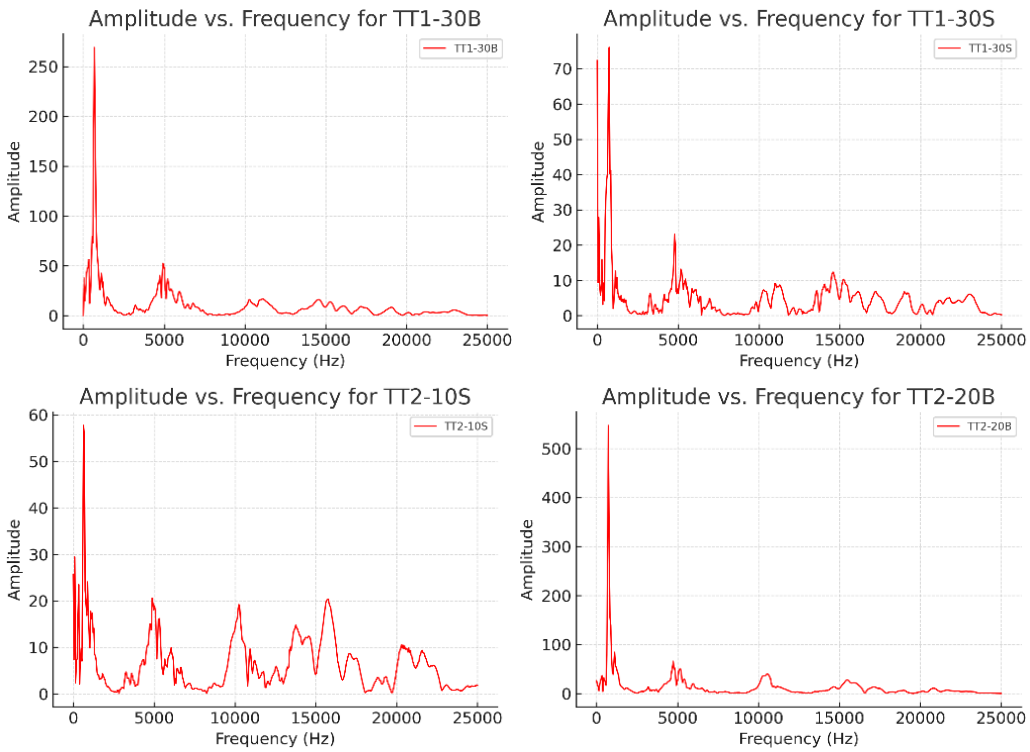

Figure 11. Amplitude vs. frequency spectrum for Line 3

Line-Wise Observations

Line 1 showed a moderate level of variation in dominant frequencies, ranging from 488 Hz to 830 Hz, which translated to concrete thickness estimates between 2.41 meters and 4.10 meters. Tests using the small hammer, especially in configurations like TT1-10S and TT1-20S, produced consistent results, pointing to generally uniform material along this section. However, the slightly lower frequency observed in TT1-30S suggested the possibility of minor internal changes or inconsistencies within the concrete. When tested with the big hammer, configurations such as TT1-20B and TT1-30B followed a similar trend. As expected, the frequency peaks were broader due to the bigger energy input, but the overall response remained stable. These outcomes suggest that while Line 1 is mostly uniform, there may be some localized areas worth closer attention.

Line 2 presented a slightly higher range of dominant frequencies, from 585 Hz to 830 Hz, indicating either thinner concrete sections or areas of increased density compared to Line 1. The calculated thickness fell between 2.41 meters and 3.41 meters. Results from small hammer tests, such as TT2-10S and TT2-20S, were largely consistent with those from Line 1, hinting at continuity in construction quality. Similarly, the big hammer tests, like TT2-30B, showed little variation, and the thickness estimates were stable throughout. Overall, Line 2 appeared to be structurally sound, with a consistent material profile and no significant signs of irregularity.

ISSN:2523 - 0522
Volume 8, Issue 2, October 2025
ISRAA UNIVERSITY JOURNAL OF APPLIED SCIENCE (IUJAS)

Line 3 stood out as the most consistent and homogeneous among the three. The dominant frequencies ranged from 634 Hz to 732 Hz, corresponding to concrete thicknesses between 2.73 meters and 3.15 meters. All tests along this line whether using the small or big hammer yielded results that were tightly grouped and showed minimal deviation. This consistency suggests a high degree of uniformity in the material properties, likely reflecting careful construction and well-controlled site conditions. Among all the areas tested, Line 3 displayed the clearest indication of stable and reliable structural performance.

Spectral Insights

The Fourier Transform analysis offered a comprehensive view of the frequency spectrum for each test configuration, shedding light on the material behavior beneath the court's surface. The presence of dominant frequency peaks in specific configurations closely aligned with the calculated thickness values, reinforcing the expected correlation between frequency and material layer depth.

In Line 1, configurations such as TT1-20S and TT1-30B exhibited well-defined peaks that corresponded to thinner regions within the concrete slab. This variation in spectral response supports earlier observations of localized differences in material composition or compaction quality along this line.

In contrast, Lines 2 and 3 displayed more consistent spectral patterns, with relatively uniform peak frequencies and amplitudes across all test setups. This uniformity suggests a greater degree of material homogeneity and indicates fewer internal irregularities in these sections. Notably, Line 3 stood out for its stability and repeatability, reflecting a well-compacted and uniformly constructed surface. The type of hammer used during testing also played a significant role in shaping the spectral characteristics. Tests performed with the big hammer consistently generated broader and higher amplitude peaks, a result of the hammer's greater energy input and deeper wave penetration. These spectral features made it easier to detect subsurface changes at greater depths but also introduced more spectral spread, particularly in areas with layered transitions or boundary irregularities. Table 2 summarizes the key results obtained from the Impact-Echo (IE) testing, providing a comprehensive overview of the subsurface conditions and material characteristics of the basketball court. By examining the dominant frequencies and their associated calculated thicknesses for each test configuration, important conclusions can be drawn regarding the structural integrity, uniformity, and

variability of the concrete slab.

A clear inverse relationship between dominant frequency and material thickness is observed throughout the results. Configurations with higher frequencies, such as TT1-20S (830.08 Hz), typically correspond to thinner or denser layers, suggesting a more compact or rigid material structure. In contrast, lower frequencies, like those found in TT2-20B (439.45 Hz), indicate thicker or less dense material regions, reflecting slower wave propagation due to lower stiffness or greater depth.

Table 2. Dominant frequencies, calculated thicknesses, and observations from Impact-Echo testing

Test Line	Dominant Frequency Range (Hz)	Thickness Range (m)	Overall Observations
Line 1	439 – 830	2.41 – 4.55	Highest variability with evidence of localized anomalies; potential internal heterogeneity in some sections.
Line 2	585 – 830	2.41 – 3.41	Moderate uniformity with minor localized variations; results generally consistent.
Line 3	634 – 732	2.73 – 3.15	Most homogeneous and stable; well-compacted material with minimal variability.

In Line 1, the data reflect a mixed structural profile, with moderate variability in both frequency and thickness. For instance, TT1-10S (488.76 Hz) corresponds to a thickness of 4.09 meters, indicating a moderately thick layer with relatively uniform properties. Meanwhile, TT1-20B (683.59 Hz) reflects a more consistent and possibly denser section. The variation across this line points to areas that may warrant further assessment to ensure consistent performance. Line 2 generally demonstrates thinner concrete layers, as evidenced by configurations like TT1-30S (830.08 Hz), supporting the interpretation of a dense and compact material composition. While the majority of readings suggest a relatively uniform profile, certain configurations such as TT2-20S (585.94 Hz) show minor deviations, potentially attributed to localized inconsistencies or differences in surface preparation. Line 3 exhibits the most consistent structural behavior among the three lines. Dominant frequencies recorded in configurations like TT1-20S (732.42 Hz) and TT2-20S (732.42 Hz) suggest a uniform and well-

compacted material layer. The moderate thickness associated with readings such as TT1-10S (634.77 Hz) reinforces the observation of stable subsurface conditions along this line.

Trends in Frequency, Thickness, and Sensor Distance

A key aspect of the analysis involved examining the relationship between sensor distance, dominant frequency, and calculated material thickness. The results consistently demonstrated that smaller sensor distances, particularly 10 cm and 20 cm tended to capture lower frequency values, which corresponded to thicker material layers. For example, in Line 1, the configuration TT1-10S recorded a frequency of 488 Hz, with a corresponding thickness of 4.10 meters, while TT1-20S showed a frequency of 585 Hz and a thickness of 3.41 meters. In contrast, tests using a sensor distance of 30 cm typically recorded higher frequencies, indicating thinner material sections. As an example, TT1-30S in Line 1 exhibited a frequency of 830 Hz, corresponding to a thickness of 2.41 meters. This pattern highlights how sensor spacing influences wave propagation, with shorter distances capturing more localized, high-detail signals, and longer distances favoring higher-frequency, surface-sensitive responses.

The type of hammer used during testing also played a role in shaping the results, as illustrated in Figure 12. Tests conducted with the big hammer generally produced higher frequencies and slightly thinner calculated thickness compared to those with the small hammer. This effect is attributed to the greater energy generated by the big hammer, which enhances wave penetration depth and influences the resonant frequency response. Despite these variations, the inverse relationship between frequency and thickness remained consistent across all test lines and configurations.

In terms of material uniformity, clear differences were observed between the three test lines. Line 3 exhibited the highest degree of consistency, with a narrow frequency range of 634–732 Hz and corresponding thicknesses between 2.73–3.15 meters. These results suggest a homogeneous material composition with minimal structural variation. In contrast, Line 1 showed the greatest variability, with frequencies ranging from 488 Hz to 830 Hz and thicknesses from 2.41 to 4.10 meters, indicating possible material heterogeneity or testing disturbances.

ISSN:2523 - 0522
Volume 8, Issue 2, October 2025
ISRAA UNIVERSITY JOURNAL OF APPLIED SCIENCE (IUJAS)

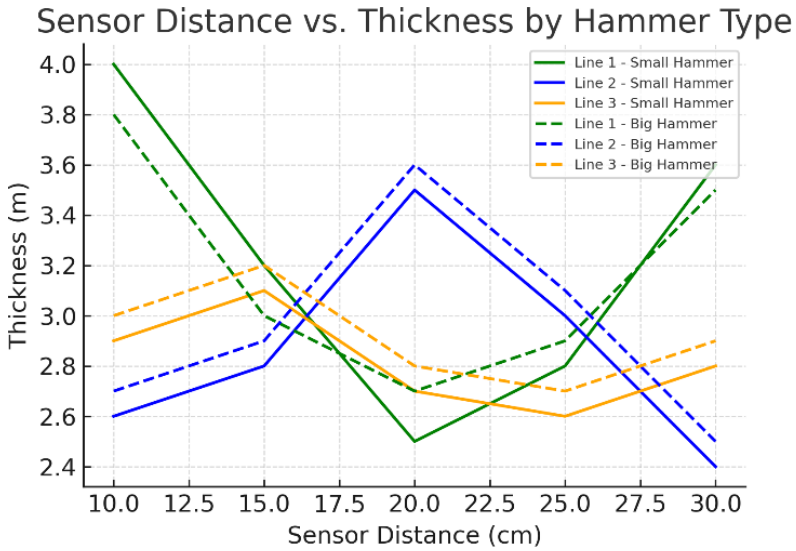

Figure 12. Sensor distance vs. thickness: variation across Lines 1–3 with small and big hammers.

Table 3 presents a summary of the frequency and thickness range observed across the three lines, along with key interpretations. The table reinforces that Line 1 is characterized by higher variability and potential inconsistencies, Line 2 displays moderate uniformity with minor localized variations, and Line 3 is the most structurally consistent, suggesting high-quality construction and uniform subsurface condition.

Table 3. Summary of Key Findings Related to Phase Angle Behavior

Aspect	Key Findings
Distance Dependency	Increasing sensor distance reduces Phase Angle magnitude and variability. Longer distances (30 cm) show smoother results (0.00002 to 0.041, mean: 0.002–0.003), while shorter distances (10 cm) show sharper peaks (0.00002 to 0.085, mean: 0.005–0.007).
Hammer Size Influence	Small hammer provides sharper peaks (e.g., 10 cm: 0.00004 to 0.068, mean: 0.005), while the big hammer gives smoother responses (e.g., 10 cm: 0.00002 to 0.085, mean: 0.006).
Line Variability	Line L1 is the most stable (0.00002 to 0.085, mean: 0.005–0.007), while Line L3 is the most sensitive to anomalies (up to 0.07, mean: 0.004–0.006). Line L2 shows moderate variability (0.0001 to 0.063, mean: 0.005–0.006).
High-Frequency Noise	Phase Angle readings become unreliable beyond 800 Hz due to noise. Reliable ranges are typically 0.00002 to 0.07 for low-to-mid frequencies (<800 Hz).

Phase Angle Behavior Analysis

ISSN:2523 - 0522
Volume 8, Issue 2, October 2025
ISRAA UNIVERSITY JOURNAL OF APPLIED SCIENCE (IUJAS)

This section explores the Phase Angle behavior observed during Impact-Echo (IE) testing across three sensor lines (L1, L2, and L3) using varying sensor distances (10 cm, 20 cm, and 30 cm) and two hammer types (small and big). The analysis is supported by visual data representations in Figures 13-18, highlighting how these variables influence phase characteristics and providing insight into subsurface consistency, wave coherence, and sensitivity to localized variations.

Understanding the relationship between Phase Angle and Frequency is essential for interpreting IE test results, as it adds an important dimension to frequency-domain analysis. The IE technique involves applying a mechanical impact to the concrete surface, generating stress waves that reflect off internal boundaries and defects. By analyzing the frequency content and phase relationships of the recorded signals, one can infer the presence of subsurface anomalies, such as delaminations, voids, or material inconsistencies.

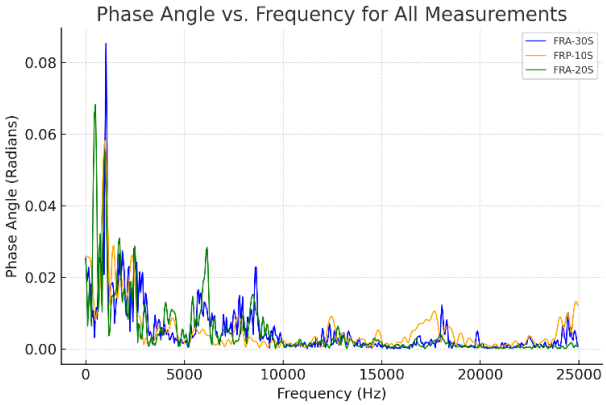

Figure 13. Phase Angle vs. frequency: Line 1 measurements using the small hammer

Incorporating Phase Angle analysis into traditional IE testing significantly enhances the ability to detect defects, especially when ambient noise or overlapping wavefronts might obscure frequency peaks. In advanced applications such as air-coupled IE methods phase spectra from multiple sensors are used to isolate frequencies that correspond to internal reflections, improving reliability and accuracy by minimizing the impact of propagating waves and environmental interference.

The distance between sensors plays a pivotal role in shaping Phase Angle behavior. At a 10 cm spacing, the Phase Angle is highly responsive to localized changes in the material. This configuration produces sharp peaks and notable variability, reflecting the method's sensitivity to fine-scale surface conditions. Across all configurations at this spacing, the Phase Angle ranged from 0.00002 to 0.085, with an average value between 0.005 and 0.007.

ISSN:2523 - 0522
Volume 8, Issue 2, October 2025
ISRAA UNIVERSITY JOURNAL OF APPLIED SCIENCE (IUJAS)

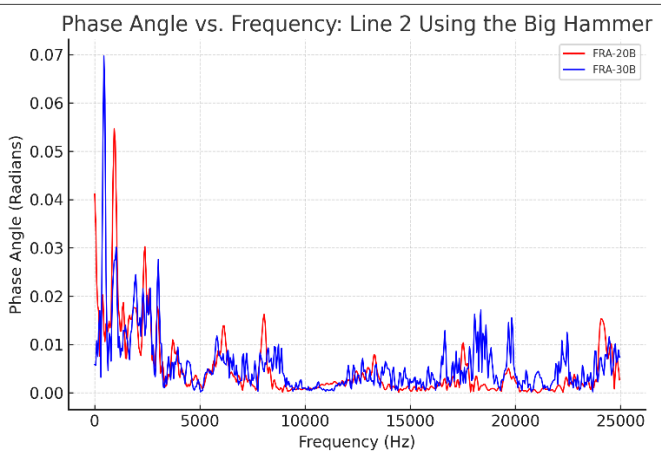

Figure 14. Phase Angle vs. frequency: Line 1 measurements using the big hammer.

At a 20 cm spacing, the Phase Angle response became more balanced. The variability decreased, and the numerical range narrowed to 0.0001 to 0.063, with a slightly more consistent average of 0.005 to 0.006. This suggests that intermediate spacing provides a good balance between sensitivity and signal stability, making it effective for identifying broader material trends without being overly affected by minor surface inconsistencies.

The 30 cm spacing produced the smoothest Phase Angle trends, with minimal fluctuation and a tightly constrained range of 0.00002 to 0.041. The average values were notably lower, falling between 0.002 and 0.003. This reduction in variability suggests that longer sensor distances dampen high-frequency noise and localized anomalies, resulting in cleaner phase data. However, this also means the system becomes less sensitive to subtle surface-level defects.

Hammer size plays a crucial role in shaping Phase Angle behavior during Impact-Echo testing. The small hammer, particularly at shorter sensor distances such as 10 cm, produces sharper peaks, making it highly effective for detecting localized ground variations. At this spacing, Phase Angle values for the small hammer ranged from 0.00004 to 0.068, with an average of approximately 0.005. However, this increased sensitivity also leads to greater noise levels, which can complicate interpretation, especially in environments with minor surface irregularities. In contrast, the big hammer generates smoother and more stable Phase Angle curves. At the same 10 cm distance, its Phase Angle value ranged from 0.00002 to 0.085, with a slightly higher mean of 0.006. The larger impact energy of the big hammer results in a more averaged response, reducing the influence of small-scale inconsistencies. At longer sensor distances, such as 30 cm, both hammers showed a

ISSN:2523 - 0522
Volume 8, Issue 2, October 2025
ISRAA UNIVERSITY JOURNAL OF APPLIED SCIENCE (IUJAS)

narrowing of Phase Angle ranges 0.00002 to 0.027 for the small hammer, and 0.00002 to 0.041 for the big hammer indicating reduced sensitivity but improved data stability. These findings suggest that the selection of hammer size should align with testing objectives: the small hammer is better suited for identifying fine-scale anomalies, while the big hammer is more appropriate for achieving stable, generalized structural assessments

Phase Angle behavior also varied noticeably across the three sensor lines (L1, L2, and L3), reflecting potential differences in subsurface conditions or sensor alignment. Line L1 exhibited the most consistent and stable Phase Angle trends across all configurations, with values ranging from 0.00002 to 0.085 and a mean between 0.005 and 0.007. This consistency suggests uniform material properties and reliable signal conditions, making Line L1 a strong baseline for comparison. Line L2 showed moderate variability, particularly at the 20 cm sensor distance, where Phase Angle values ranged from 0.0001 to 0.063, with an average between 0.005 and 0.006..

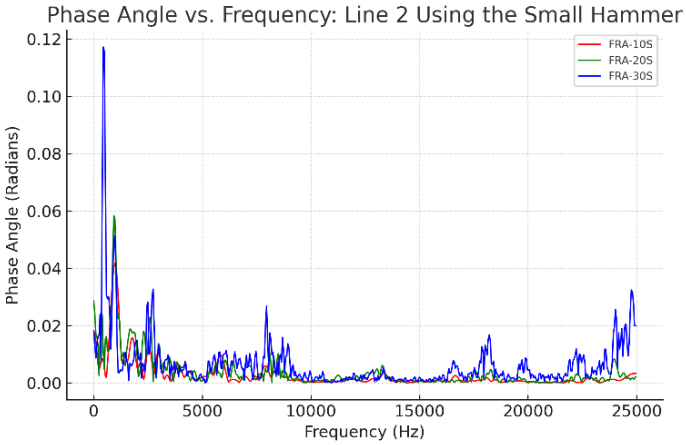

Figure 15. Phase Angle vs. Frequency: Line 2 measurements using the big hammer.

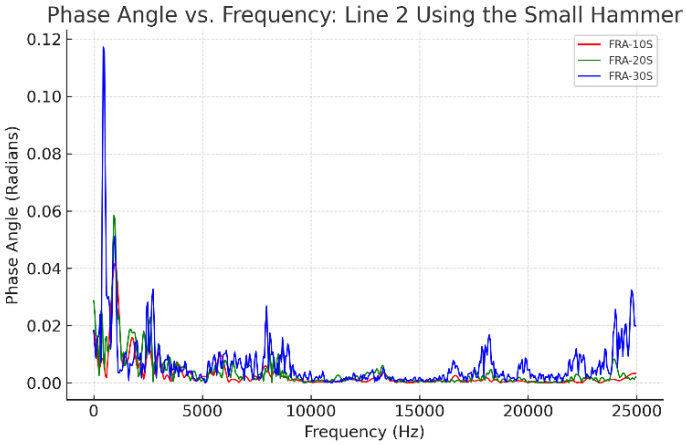

Figure 16. Phase Angle vs. Frequency: Line 2 measurements using the small hammer

ISSN:2523 - 0522
Volume 8, Issue 2, October 2025
ISRAA UNIVERSITY JOURNAL OF APPLIED SCIENCE (IUJAS)

This suggests a relatively stable profile with occasional deviations, possibly due to minor material inconsistencies or surface texture differences. In contrast, Line L3 demonstrated the highest sensitivity to anomalies. This was especially evident when using the small hammer at 10 cm spacing, where the Phase Angle showed more pronounced fluctuations, with peaks reaching up to 0.07. The sharper, more irregular trends observed in Line L3 may reflect localized ground irregularities or slight misalignments in sensor positioning. While such sensitivity is advantageous for detecting early signs of structural anomalies, it also necessitates cautious interpretation to differentiate real material variations from signal noise.

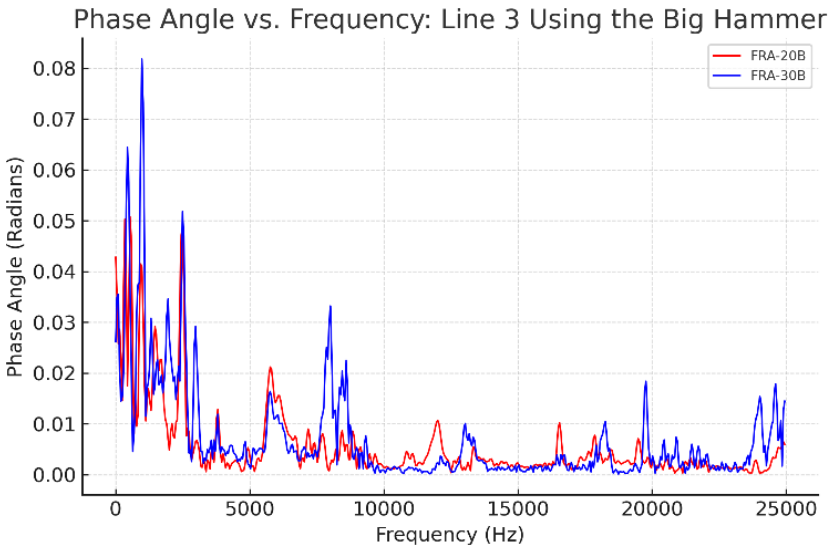

Figure 17. Phase Angle vs. Frequency: Line 3 measurements using the big hammer.

The reliability of Phase Angle measurements significantly decreases at high frequencies (greater than 800 Hz), where the influence of signal noise becomes more pronounced. In this range, Phase Angle values tend to fluctuate unpredictably, reducing their usefulness for accurate interpretation. By contrast, in the low-to-mid frequency range (below 800 Hz), Phase Angle behavior is generally stable and consistent, making it a more reliable domain for structural analysis. Across all test configurations, Phase Angle values within this frequency range typically fall between 0.00002 and 0.07, providing robust and interpretable data for evaluating subsurface conditions.

High-frequency noise is especially noticeable at shorter sensor distances, such as 10 cm, and is most prominent in Line L3, where localized material irregularities contribute to erratic signal behavior.

These conditions amplify fluctuations in the Phase Angle, further complicating analysis in high-frequency regions.

Table 4 summarizes the key observations regarding Phase Angle trends during Impact-Echo testing, emphasizing the roles of sensor distance, hammer type, and sensor line variability. The data clearly show that increasing the sensor spacing leads to a reduction in Phase Angle magnitude and variability. At 30 cm, results are smoother and more stable, whereas at 10 cm, sharper peaks are common due to increased sensitivity to near-surface features. Similarly, the small hammer generates more pronounced peaks in the Phase Angle response, suitable for detecting localized anomalies, while the big hammer produces broader and smoother trends, better suited for general assessments. Among the three sensor lines, Line L1 remains the most stable and consistent, whereas Line L3 exhibits the highest sensitivity, reflecting both its diagnostic potential and its susceptibility to environmental or surface-induced noise.

Table 4. Summary of Key Findings Related to Phase Angle Behavior

Aspect	Key Findings
Distance Dependency	Increasing sensor distance reduces Phase Angle magnitude and variability. Longer distances (30 cm) show smoother results (0.00002 to 0.041, mean: 0.002–0.003), while shorter distances (10 cm) show sharper peaks (0.00002 to 0.085, mean: 0.005–0.007).
Hammer Size Influence	Small hammer provides sharper peaks (e.g., 10 cm: 0.00004 to 0.068, mean: 0.005), while the big hammer gives smoother responses (e.g., 10 cm: 0.00002 to 0.085, mean: 0.006).
Line Variability	Line L1 is the most stable (0.00002 to 0.085, mean: 0.005–0.007), while Line L3 is the most sensitive to anomalies (up to 0.07, mean: 0.004–0.006). Line L2 shows moderate variability (0.0001 to 0.063, mean: 0.005–0.006).
High-Frequency Noise	Phase Angle readings become unreliable beyond 800 Hz due to noise. Reliable ranges are typically 0.00002 to 0.07 for low-to-mid frequencies (<800 Hz).

DISCUSSION

The analysis and findings of this research underscore the value of combining Fourier Transform and Phase Angle behavior analysis to evaluate the subsurface conditions of concrete basketball court flooring. Vibrational data collected from three distinct sensor lines (Lines 1, 2, and 3) revealed critical insights into material properties, structural uniformity, and potential variability. By examining the combined influence of hammer type, sensor distance, and ground response, a detailed understanding of the surface's structural integrity was achieved.

ISSN:2523 - 0522
Volume 8, Issue 2, October 2025
ISRAA UNIVERSITY JOURNAL OF APPLIED SCIENCE (IUJAS)

The Fourier Transform analysis (Figures 9–11) identified notable variations in frequency and corresponding thickness across the three sensor lines. As shown in Table 4, Line 1 exhibited the greatest variability, with thickness values ranging from 2.41 to 4.55 m and dominant frequencies between 488 Hz and 830 Hz. These variations suggest potential material heterogeneity and possible localized defects, particularly evident in configurations such as TT1-30S, which display irregular internal reflections. In contrast, Line 2 demonstrated a higher degree of uniformity, with dominant frequencies between 585 Hz and 830 Hz and thicknesses ranging from 2.41 to 3.41 m. Although generally consistent, some configurations, like TT2-20S, indicated minor localized inconsistencies. Line 3 proved to be the most homogeneous section, with a narrow frequency range of 634–732 Hz and consistent thicknesses between 2.73 and 3.15 m, reflecting superior material uniformity and minimal internal variability.

Table 5. Comparison of Results Across Sensor Lines

Line	Thickness Range (m)	Material Homogeneity	Phase Angle Behavior
1	2.41 – 4.55	High variability; potential heterogeneity and anomalies	Stable but more sensitive to anomalies at short distances
2	2.41 – 3.41	Moderate uniformity; occasional minor variations	Moderate variability at mid distances; balanced response
3	2.73 – 3.15	High consistency; superior material homogeneity	Most stable and consistent across all sensor distances

Comparative evaluation of the three lines (Figure 12; Table 4) reveals clear structural differences. Line 1 displayed the highest variability and raised concerns about material inconsistencies and potential structural weaknesses. Line 2 served as a transitional zone, balancing the irregularities observed in Line 1 with the stability of Line 3. Meanwhile, Line 3 stood out as the most reliable and structurally sound area, with consistent responses across all configurations. These differences highlight the importance of conducting line-specific analysis when assessing large concrete surfaces to detect and address localized issues that may affect overall performance (Li et al., 2024).

The Phase Angle analysis (Figures 13–18; Table 3) complemented the frequency-domain findings by providing a deeper look at wave behavior across configurations. An increase in sensor spacing was shown to reduce Phase Angle fluctuations, producing smoother, more stable responses while reducing sensitivity to localized anomalies. The small hammer yielded sharper peaks in the Phase Angle data, proving useful for identifying fine-scale surface defects, whereas the big hammer generated broader,

less noise-sensitive curves, offering reliable insights into general structural conditions.

Across the three sensor lines, Line 3 showed the highest sensitivity to anomalies, especially at shorter distances and with the small hammer (Figure 16). This suggests that while Line 3 is structurally consistent, it is also effective for detecting subtle changes, making it an ideal candidate for monitoring material performance over time. Line 1, on the other hand, demonstrated the most stable Phase Angle behavior, despite its underlying material variability, reinforcing its role as a structural baseline.

The practical implications of these findings are significant for the ongoing maintenance and management of sports infrastructure. The uniformity observed in Line 3 suggests that this section is well-compacted and structurally sound, requiring minimal intervention. Conversely, the variability in Line 1 indicates areas that may require further investigation, potential reinforcement, or targeted maintenance. Areas associated with higher frequencies and thinner layers, particularly in Lines 2 and 3, may be more susceptible to stress concentrations and wear overtime, warranting periodic monitoring.

CONCLUSIONS

This study has demonstrated the effectiveness of the Impact-Echo (IE) method in evaluating the material uniformity and structural integrity of basketball court flooring. By integrating Fourier Transform and Phase Angle analysis, the research offers valuable insights into wave propagation behavior, the presence of subsurface anomalies, and the impact of variables such as sensor distance and hammer type on measurement precision. The findings clearly indicate that Line 1 exhibits substantial material variability, pointing to potential structural inconsistencies, whereas Line 2 reflects moderate uniformity. In contrast, Line 3 emerges as the most homogeneous and structurally sound section, suggesting a stable and well-compacted surface.

The Phase Angle analysis further emphasizes the sensitivity of wave behavior to testing conditions. Shorter sensor distances and the use of small hammers enhance the detection of localized defects, while longer distances and bigger hammers yield smoother and more stable responses. These observations highlight the importance of carefully selecting and optimizing IE test parameters to ensure accurate, repeatable, and reliable nondestructive evaluations, particularly for thin concrete structures in sports infrastructure. In addition, frequency-domain analysis proved effective for identifying variations in material thickness, supporting improved assessments of layer uniformity and

subsurface consistency.

From a practical perspective, these findings can inform the development of standardized IE testing protocols for sports facilities, helping engineers and facility managers detect early-stage defects, maintain consistent playing surfaces, and reduce the risk of sudden failures that could compromise athlete safety. Explicitly linking IE test outputs to maintenance schedules could improve lifecycle management and align with emerging nondestructive testing standards in concrete diagnostics.

Looking ahead, future research should aim to refine testing configurations to further enhance the accuracy and reliability of the IE method for sports applications. Investigating alternative sensor placements, varying impact energies, and different excitation methods could improve sensitivity and detection resolution in thin concrete layers. Developing these approaches may lead to a standardized framework for assessing material properties and detecting subsurface anomalies in basketball courts and similar installations. Another key area for future exploration is the long-term analysis of material degradation, particularly how cyclic loading, environmental exposure, and surface wear influence the structural performance of sports flooring. Regular monitoring of these factors through periodic nondestructive testing could support predictive maintenance strategies, reduce long-term repair costs, and ensure continued safety and usability.

Furthermore, deeper investigation is needed to establish a direct correlation between IE test results and intrinsic concrete properties, including density, porosity, and microcracking behavior. Gaining a better understanding of these relationships would improve the diagnostic accuracy of condition assessments and support the development of quantitative indicators for material performance. This would be especially useful for identifying microstructural changes that may precede visible surface damage, allowing for early intervention and better lifecycle management of sports infrastructure.

ACKNOWLEDGMENTS

The authors would like to express their sincere gratitude to Universitas Muhammadiyah Yogyakarta (UMY) for providing continuous support throughout this research. The facilities, resources, and academic environment offered by UMY were instrumental in completing this study. The authors also extend their appreciation to colleagues and collaborators who contributed valuable insights and encouragement during the course of this work.

REFERENCE

1. Afanda, R., & Zaki, A. (2025). Effects of repair grouting and jacketing on corrosion concrete using ultrasonic method. *SDHM Structural Durability and Health Monitoring, 19*(2), 265–284. https://doi.org/10.32604/sdhm.2024.053084
2. Apostolopoulos, C. A. (2010). Coastal bridges and the 120 life span – The Rio-Antirio case study. *International Journal of Structural Integrity, 1*(2). https://doi.org/10.1108/17579861011053907
3. Bahati, P. A., Le, V. D., & Lim, Y. (2021). An impact echo method to detect cavities between railway track slabs and soil foundation. *Journal of Engineering and Applied Science, 68*(1). https://doi.org/10.1186/s44147-021-00008-w
4. Dethof, F., Algernon, D., Thurnherr, C., & Keßler, S. (2024). Factors influencing impact echo simulations in thick concrete structures. *Journal of Advanced Concrete Technology, 22*(10), 636–649. https://doi.org/10.3151/jact.22.636
5. Dvořák, R., & Topolář, L. (2021). Effect of hammer type on generated mechanical signals in impact-echo testing. *Materials, 14*(3), 606. https://doi.org/10.3390/ma14030606
6. Ge, J., Yang, C., Yu, F., & Yusa, N. (2022). Transformation of the rotating eddy current testing signal at the desired eddy current orientation. *NDT & E International, 125*, 102551. https://doi.org/10.1016/j.ndteint.2021.102551
7. Joh, S. H. (1996). *Advances in the data interpretation technique for spectral-analysis-of-surface-waves (SASW) measurements* (Doctoral dissertation).
8. Kee, S. H., Lee, J. W., & Candelaria, M. D. (2020). Evaluation of delamination in concrete by IE testing using multi-channel elastic wave data. *Sensors, 20*(1), 201. https://doi.org/10.3390/s20010201
9. Kim, D. H., Choi, M. K., Han, S. H., & Jeong, J. H. (2022). Determination of partial depth repair size for spalling of jointed concrete pavements using the impact echo method. *Sustainability, 14*(13), 8143. https://doi.org/10.3390/su14138143
10. Kouddane, B., Sbartaï, Z. M., Alwash, M., Ali-Benyahia, K., Elachachi, S. M., Lamdouar, N., & Kenai, S. (2022). Assessment of concrete strength using the combination of NDT—Review and performance analysis. *Applied Sciences, 12*(23), 12190. https://doi.org/10.3390/app122312190
11. Li, C., Su, R. K. L., & Pan, X. (2024). Assessment of out-of-plane structural defects using parallel laser line scanning system. *Computer-Aided Civil and Infrastructure Engineering, 39*(6), 669–683. https://doi.org/10.1111/mice.13102
12. Lin, H. C., & Ye, Y. C. (2019). Reviews of bearing vibration measurement using fast Fourier transform and enhanced fast Fourier transform algorithms. *Advances in Mechanical Engineering, 11*(1), 1–11. https://doi.org/10.1177/1687814018816751
13. Lu, J. X., Shen, P., Zheng, H., Ali, H. A., & Poon, C. S. (2021). Development and characteristics of ultra high-performance lightweight cementitious composites (UHP-LCCs). *Cement and Concrete Research, 145*, 106462. https://doi.org/10.1016/j.cemconres.2021.106462
14. Noshahri, H., Wijnant, Y., Cernat, C., Dertien, E., & Scholtenhuis, L. O. (2021). Comparison of sensors for contactless detection of void behind concrete using stress waves. In *2021 IEEE Sensors Applications Symposium (SAS)* (pp. 1–6). IEEE. https://doi.org/10.1109/SAS51076.2021.9530111
15. Sansalone, M., & Streett, W. B. (1997). *Impact-echo: Nondestructive testing of concrete and masonry*. Ithaca, NY: Bullbrier Press.
16. Sawicki, B., Piotrowski, T., & Garbacz, A. (2021). Development of impact-echo multitransducer device for automated concrete homogeneity assessment. *Materials, 14*(9), 2144.

https://doi.org/10.3390/ma14092144

17. Scherr, J. F., & Grosse, C. U. (2021). Delamination detection on a concrete bridge deck using impact echo scanning. *Structural Concrete, 22*(2), 1169–1180. https://doi.org/10.1002/suco.202000415
18. Scherr, J. F., Kollofrath, J., Popovics, J. S., Bühling, B., & Grosse, C. U. (2023). Detection of delaminations in concrete plates using a laser ablation impact echo technique. *Journal of Nondestructive Evaluation, 42*(1), 1–12. https://doi.org/10.1007/s10921-022-00921-x
19. Wang, B., & Gupta, R. (2021). Analyzing bond-deterioration during freeze-thaw exposure in cement-based repairs using non-destructive methods. *Cement and Concrete Composites, 115*, 103830. https://doi.org/10.1016/j.cemconcomp.2020.103830
20. Yu, J., Liu, D., & Zhang, Z. (2022). Durability and life prediction analysis of recycled aggregate concrete with ceramic waste powder under freeze-thaw conditions based on impact-echo method and Grey-Markov model. *Frontiers in Materials, 9*, 1060294. https://doi.org/10.3389/fmats.2022.1060294